INTERNATIONAL JOURNAL OF AUTOMOTIVE AND MECHANICAL ENGINEERING (IJAME)
ISSN: 2229-8649 e-ISSN: 2180-1606
VOL. 20, ISSUE 1, 2023, 10192 – 10210
DOI: https://doi.org/10.15282/ijame.20.1.2023.04.0789

ORIGINAL ARTICLE

Numerical Study of Dynamic Hydroplaning Effects on Motorcycle Tires

P. Meethum[1,2] and C. Suvanjumrat[1,2,*]

[1]Department of Mechanical Engineering, Faculty of Engineering, Mahidol University, Salaya, Nakhon Pathom 73170, Thailand
[2]Laboratory of Computer Mechanics for Design (LCMD), Department of Mechanical Engineering, Faculty of Engineering, Mahidol University, Salaya, Nakhon Pathom 73170, Thailand

ABSTRACT – Hydroplaning is a hydrodynamic phenomenon and has crucial effects on motorcycle tires that roll on a wet road at high speed. It causes an accident that results in numerous injuries and deaths of motorcyclists. This accident happens to an overestimation of the dynamic tire performance. Therefore, this research aims to propose a mathematical model to predict the maximum hydroplaning speed of motorcycle tires. The motorcycle tire was experimentally performed the hydroplaning test by the developing machine. The fluid-structure interaction (FSI), in which a rolling tire interacted with fluid on the road, was modeled using finite element and finite volume methods. It compared against the experiment and was in good agreement. Therefore, motorcycle tire hydroplaning was studied by varying velocities, inflation pressures, and carrying loads. It was found that the hydroplaning speeds had a serious relationship only to the carrying loads. Therefore, the novel function of hydroplaning velocity was established in the carrying load form. It is simple to specify the maximum hydroplaning speed of motorcycle tires. In addition, it will be a good and novel guidance tool for motorcycle riding communities and motorcycle tire manufacturers to calculate hydroplaning resistance of their motorcycle tires.

ARTICLE HISTORY
Received: 19th May 2022
Revised: 10th Jan 2023
Accepted: 01st Mar 2023
Published: 30th Mar 2023

KEYWORDS
Hydroplaning;
Motorcycle;
Tire;
Fluid-structure interaction

INTRODUCTION

Hydroplaning significantly affects tires that roll on a wet road at high speeds. Therefore, dynamic tire performance should contemplate hydroplaning inevitably. The retarding force developed on the pneumatic tire, which had rolled on the water, was proportional to the speed of the pneumatic tire initially derived by Horne et al. [1]. The aircraft tire type VII, 32×8.8 22 ply-rating rib-tread patterns, had been employed for the experimental test to verify the force equation. Two inflation pressures consisting of 792.89 and 2413 kPa, varying velocities from 109.27 to 192.61 km/hr, weighting a constant vertical load of 40.82 kN on an aircraft tire, were tire testing conditions. The depth of water prepared varies between 7.62 and 38.10 mm. They found that data obtained by the force equation were in reasonable agreement with experimental data when using drag coefficients between 0.70 and 0.75. Horne and Leland [2] experimentally studied the tread pattern of this aircraft tire and runway surface conditions, which affected braking friction and rolling resistance. They found that the circumference-groove tread developed the highest value of friction coefficient while the smooth and dimple tire tread produced the lowest values for the investigation. Horne and Dreher [3] discussed the phenomena of tire hydroplaning in their previous works. The hydroplaning conditions were partial and total development of the rolling tire. As tire speeds increased at partial hydroplaning, inertia effects tended to retard fluid escape in the tire-road contact region, and the fluid wedge then formed to detach the tire from the road surface. The hydrodynamic pressure force, which developed under the tire, was equal to the vehicle weight acting on the tire. This force completely lifted the tire off the road surface when the vehicle speeds further increased, and the total hydroplaning happened. The critical speed where the vertical force was equal to the hydrodynamic pressure force was the tire hydroplaning speed. Experimental setup of tire hydroplaning is a vast consequence and leads to a higher price. Moreover, it is difficult to control the surrounding conditions and dangerous to perform the tire test by a driver.

Because loss of laboratory testing, a computational method plays a role in modeling the tire hydroplaning instead of the field experiments. The numerical method, finite element method (FEM), often solves the hydroplaning problem. Zmindak and Grajciar [4] simulated the hydroplaning of tires with commercial software (ADINA). Because the finite element model of tire hydroplaning had limited by available computer power, the car tire was then modeled only one quarter with coarse meshes of quadratic shell elements. The tire tread model used three-dimensional elements and assumed the elastic material to represent the hyperelastic behavior of the rubber compound because it happened with less strain on the contact surface. The investigation of stresses on the tire structure was not the purpose. Four-node-tetrahedron linear elements had been discretized in the fluid domain, which separated from the tire tread. The finer mesh would perform in the groove and corner regions. In the transition region, more coarse meshes were possible. The arbitrary Lagrangian-Eulerian (ALE) formulation was used to describe fluid forming between the flexible tire and the undeformed or rigid road. Nakajima et al. [5, 6] presented a reliable numerical procedure to simulate the hydroplaning phenomenon on the automobile tire model P205/55R16. Fluid-structure interaction (FSI) between water and rolling tires used generally coupling finite volume method (FVM) and the explicit FEM with the Eulerian-Lagrangian coupling method (the same as

*CORRESPONDING AUTHOR | C. Suvanjumrat | ✉ chakrit.suv@mahidol.ac.th

ALE method) to describe water flow and tire deformation. Their FSI model would verify by comparing the simulation and measurement of water flow obtained by photography under the glass plate that supported the rolling tire on the water. Cho et al. [7] also represented the numerical procedure of the complex tire hydroplaning model, which was automobile tire model P205/60R15, for investigation. Sapragonas et al. [8] developed tire hydroplaning models using commercial explicit finite element software, MSC.PATRAN and MSC.DYTRAN. The FSI model efficiently used the Eulerian-Lagrangian coupling method. A simplified-tire model 175/65R14 had performed to investigate the effects of speeds and water film heights. They found that the grip on the pavement loosed at the tire speed of and film height of 110 km/hr and 10 mm, respectively. Jeong and Jeong [9] used explicit finite element commercial software, LS-DYNA, to model tire hydroplaning for the skid resistance study according to the ASTM E274 test method. Zhu et al. [10] used explicit FEM of ABAQUS software to model hydroplaning of an aircraft tire, 46×17.0R20, to study aviation safety during the landing stage. It was the Eulerian-Lagrangian coupling method as well. Tires of aircraft running on the wet runway would hydroplane and also spray. It might lead to a compressor stall, surge, or even combustion flameout. Zhang et al. [11] used the coupling method between smooth particle hydrodynamics (SPH) and FEM in LS-DYNA software to model the tire spray. As mentioned in the literature, tire hydroplaning utilized the Eulerian-Lagrangian coupling method for modeling. However, it might have some mysterious methodology which did not manifestly publish. Therefore, the tire hydroplaning model should verify in this research for complete knowledge.

Motorcycles on the road are increasing rapidly. One of the reasons for the increase in motorcycle usage is the compact size which permits parking motorcycles in small places. It also assists motorcycles in riding in and out of traffic easily. Motorcycles have two wheels, which are small contact patch areas of tires, and can lose control more easily than cars due to driving at high speeds on the wet road surface. Consequently, the contact-patch area between the tire and pavement is significant to be a tool for indicating the riding performance of the motorcycle and other vehicles. It should note that the contact patch can estimate the contact pressure interacting between the tire and pavement [12]. Many previous works attempted to measure and study the contact patch of each tire type. A pressure measurement film was inserted between the tire and the floor to achieve tire footprint by pressing the tire against the floor. The tire footprint on the film was converted to the contact pressure contour using the image processing technique. The contact pressure could then investigate under the increase of compression load [13]. Liu et al. [14] modeled the crown contour of a 2.75-18 motorcycle tire by FEM. The contact patch shapes had investigated to improve the grip performance of a motorcycle tire. In the above literature, the motorcycle tires lack to study their performance by modeling while they had used very much on the road.

As above numerical studies, there have been few simulation results validated against the experimental hydroplaning. Although, some research had a reliable finite element model of tire hydroplaning. Nevertheless, researchers never studied hydroplaning on motorcycle tires by experimental and numerical methods. This research would study the effect of hydroplaning on the 2.50-17 motorcycle tires that are used substantially. The FSI model of a rolling motorcycle tire on a wet road would perform to investigate the hydrodynamic force or the hydroplaning force. The speed, inflation pressure, and carrying load were varied to observe their effects. In addition, the hydroplaning testing machine was developed to experiment and benchmark with the simulation. After the reasonable simulation succeeded, the hydroplaning speeds of motorcycle tires were derived and formulated. This novel model is a good guidance tool for the dynamic performance design and manufacture of motorcycle tires. Furthermore, it utilizes motorcycle tire users and motorcycle communities that drive a motorcycle in wet driving conditions.

MODELS OF THE TIRE HYDROPLANING SPEED

The tire-ground frictional spin-up moment vanishes, and the runway fluid entirely supports the tire. The vertical component of the hydroplaning force is equal to the ground force when the tire hydroplaning exits [2, 3]. It is like the lift force acting on the airfoil angles against the airflow [15, 16]. Therefore, the force acting on tires caused by the hydroplaning is written by the following equation.

$$F_h = \frac{1}{2} C_L \rho A V_h^2 \tag{1}$$

where F_h is the hydroplaning force, C_L is lift coefficient, ρ is the fluid density, A is the tire-ground contact area, and V_h is the hydroplaning tire speed. The rearrangement of Eq. (1) leads to the following equation.

$$V_h = \sqrt{\left(\frac{F_h}{A}\right)\left(\frac{2}{C_L \rho}\right)} \tag{2}$$

The gross footprint pressure (p_C) is a variable in Eq. (2) exerted by the tire on the ground. It can be written as follows:

$$p_C = \frac{F_h}{A} \tag{3}$$

The gross footprint pressure is normally related to the inflation pressure of tires. It obtains by performing the contact patch testing. Therefore, the hydroplaning tire speed equation can be written in the inflation pressure form.

MOTORCYCLE TIRE HYDROPLANING MODEL

Governing Equations

The following equation governs the rolling tire at the current time and various boundary conditions.

$$\rho\dot{\boldsymbol{V}} = \sigma\boldsymbol{V} + \rho\boldsymbol{f} \tag{4}$$

where σ is Cauchy stress, ρ is the mass density, and $\boldsymbol{f}$ is the body force of the tire.

The tire deformation, which happens on rubber, is governed by the hyperelastic material model. The penalized first-order Mooney-Rivlin model will use for the tire hydroplaning model. It is formulated by the strain energy function as follows:

$$W(J_1, J_2, J_3, K) = C_{10}(J_1 - 3) + C_{01}(J_2 - 3) + \frac{1}{K}(J_3 - 1)^2 \tag{5}$$

where J_i is the invariant of the Green-Lagrangian train tensor, C_{10} and C_{01} are the rubber material constants, and K is a sort of penalty parameter controlling the rubber compressibility.

Boundaries where conditions of displacement boundary (Ω_x), contact boundary (Ω_c), and traction boundary (Ω_τ) are applied. Therefore, boundary conditions write as follows:

$$x(X,t) = g(X,t) \quad on\ \Omega_x \tag{6}$$

$$(x^1 - x^2) \cdot n^1 \leq 0 \ \ on\ \Omega_c \tag{7}$$

$$\sigma \cdot n = \tau \qquad on\ \Omega_\tau \tag{8}$$

where x is the displacement and t is time.

The fluid domain (Ω_f) consists of air and water. The viscous effect and the temperature change of water are negligible. Therefore, the incompressible multi-phase flow is employed to consider. The fluid flow is governed by the continuity equation and momentum equation as follows:

$$\nabla \cdot \boldsymbol{V} = 0 \tag{9}$$

$$\rho_f \frac{\partial \boldsymbol{V}}{\partial t} + \rho_f(\mathbf{V} \cdot \nabla)\boldsymbol{V} = -\nabla p \tag{10}$$

where ρ_f is the fluid density, $\boldsymbol{V}$ is velocity, and p is the hydrodynamic pressure.

The volume fraction (F) of water tracks the water surface will represent by the following transport equation [17].

$$-\nabla p \ \ \frac{\partial F}{\partial t} + \boldsymbol{V} \cdot \nabla F = 0 \tag{11}$$

In this study, the general Eulerian-Lagrangian coupling in MSC.DYTRAN has been used to model the FSI between water on the road and the tire [18].

Discretization

The explicit finite element method discrete equation of motion for a rolling tire on the road. It is written by the matrix equation as follows:

$$M\ddot{\boldsymbol{x}} + C\dot{\boldsymbol{x}} + K\boldsymbol{x} = F_n^{ext} \tag{12}$$

Equation (12) can write as follows:

$$M\ddot{\boldsymbol{x}} = F^{ext} - F^{int} \tag{13}$$

$$F^{int} = C\dot{\boldsymbol{x}} + K\boldsymbol{x} \tag{14}$$

where F^{ext} is the vector of externally applied loads, F^{int} is the vector of internally applied loads, and M is the mass matrix.

The acceleration can be found by inverting the mass matrix and multiplying it by the residual load vector (F^{res}). If the mass matrix equation is a set of independent equations for each degree of freedom, it writes as follows:

$$\ddot{\boldsymbol{x}}_i = M_i^{-1} F_i^{res} \tag{15}$$

$$F_i^{res} = F_i^{ext} - F_i^{int} \tag{16}$$

The central difference scheme will use to advance in time then the velocity and displacement of a rolling tire can write as follows:

$$\dot{\boldsymbol{x}}_{n+1/2} = \dot{\boldsymbol{x}}_{n-1/2} + \ddot{\boldsymbol{x}}_n \frac{\left(\Delta t_{n+1/2} - \Delta t_{n-1/2}\right)}{2} \tag{17}$$

$$\boldsymbol{x}_{n+1} = \boldsymbol{x}_n + \dot{\boldsymbol{x}}_{n+1/2} \Delta t_{n+1/2} \tag{18}$$

According to the discretization of the motion equation, the motorcycle tire model depicted in Figure 1. This finite element model was developed from the computational-aided design (CAD) model of a motorcycle tire series ND-300 by N.D. Rubber Public Co., Ltd. This 2.25-17 tire had an outside diameter of 553.00 mm. Meanwhile, its width was 61.00 mm. The tread pattern of this tire caused the depth of the groove to be 4.5 mm. All elements of the tire component were solid elements. The wire, belt, and rubber elements were hexahedral, and the tread elements were tetrahedral. Four levels of element number for the motorcycle tire model consisting of 95999, 162209, 271136, and 421607 elements were performed in the convergent test. The constant value of contact force was used to define the stability of the element number. Figure 2 shows the result of the mesh independence study. It found that the stability of the simulated results was obtained at the total tire elements of 271136. The results of the finite element analysis (FEA) were not affected by the increase in element number to 421607. The tire model is assembled with the road model, as shown in Figure 3. The road model was created by the shell elements or plate elements. Their shape was quadrilateral and had a total number of 3703 elements. Before the tire model rolled on the runway, it would inflate by the constant air pressure. Subsequently, the tire model supported the carrying loads consisting of a rider and motorcycle. These loads, which acted on the tire, were separated into two steps. Finally, the tire rolled on the runway with a constant translational velocity while carrying these loads. This translational velocity of the rolling tire corresponded to the rotation velocity. The contact algorithm was assigned to the tire and runway surface models. It caused the motorcycle tire not to penetrate the runway model. The air inflation pressure, carrying load, velocities, and contact algorithm were the boundary conditions of this rolling tire model. The ground force, which was calculated by the rolling tire on the road model, was a significant result. It was anticipated to be variable by varying the inflation pressures, carrying loads, or velocities.

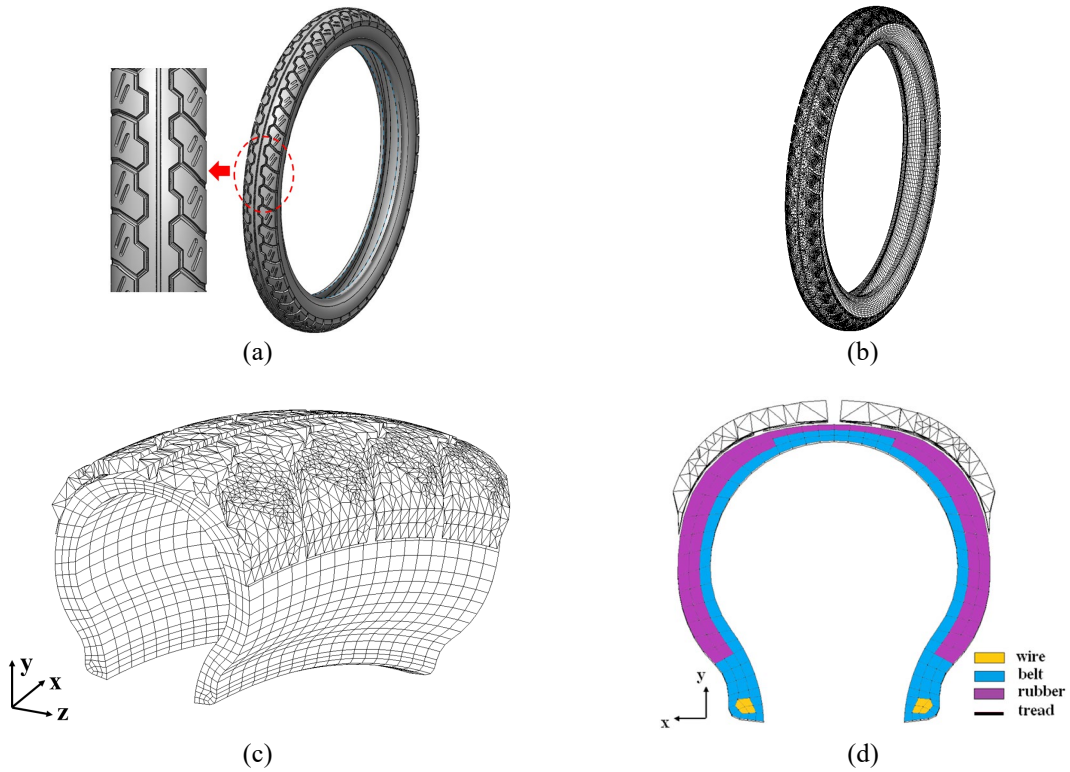

Figure 1. The models of the 2.25-17 motorcycle tire consisting of (a) the CAD model, (b) the 3-D full-scale finite element model, (c) the cross-section, and (d) detailed elements of finite element model

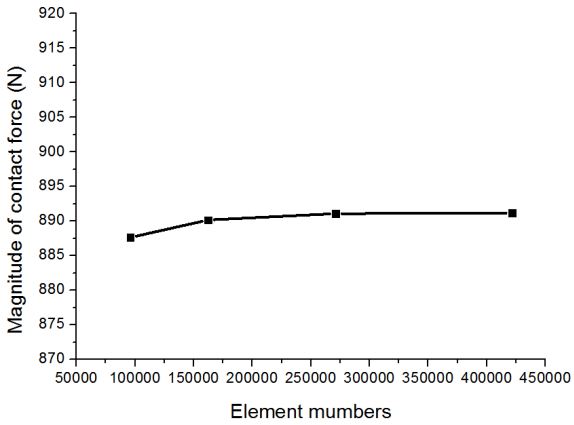

Figure 2. The mesh convergence testing result

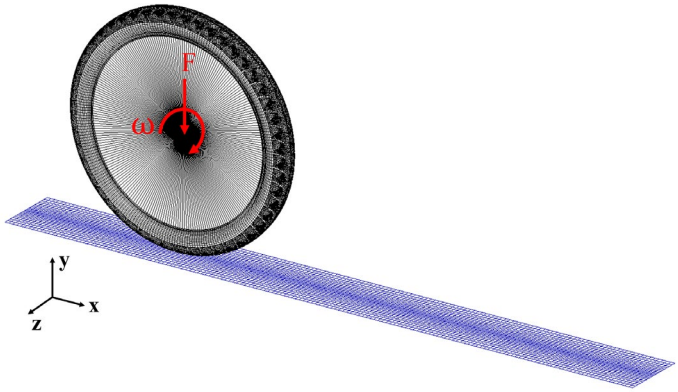

Figure 3. The finite element model of the rolling tire on the road

Motorcycle Tire Rolling on the Wet Road

The fluid domain is the fixed domain. The finite volume method uses to discrete its cell structure. The interested cell has node P, which shares its surfaces with neighboring cells. The fluid properties such as velocity and pressure calculate at a node of cells. The FVM discretizes the transient continuity and momentum equations of incompressible flow. Therefore, the explicit form of the discretized equation can write as follows:

$$a_p^{t+\Delta t}\emptyset_p^{t+\Delta t} = a_p^t\emptyset_p^t + \sum_{nb} a_{nb}\emptyset_{nb} + S_\emptyset \tag{19}$$

$$a_p^{t+\Delta t} = a_p^t = \rho_f \frac{\Delta \forall}{\Delta t} \tag{20}$$

where a_p is the coefficient of variable at an interesting node, a_{nb} is the coefficient of variable at neighbouring nodes, $\emptyset_p$ is the fluid properties at an interesting node, $\emptyset_{nb}$ is the fluid properties at neighboring nodes, and $\forall$ is the volume of cell.

In the tire hydroplaning model, the cell structure of the fluid domain that covers the contact surface between the tire and the road depicts in Figure 4. It used the hexahedron cells to create the Euler domain. This study had a total fluid cell of 35200 cells. The cells on the water surface would be smaller than in other areas. This study assigned the constant height of water at 3.00 mm. Therefore, the water and air cells were 7040 and 28160, respectively. The interaction between tire and water on the road will happen and governs by the following equations.

$$-p\boldsymbol{I}\cdot\boldsymbol{n}_f = \boldsymbol{\sigma}\cdot\boldsymbol{n}_s \tag{21}$$

where p is the hydrodynamic pressure, $\boldsymbol{I}$ is the unit tensor, the f subscript is fluid, and the s subscript is tires.

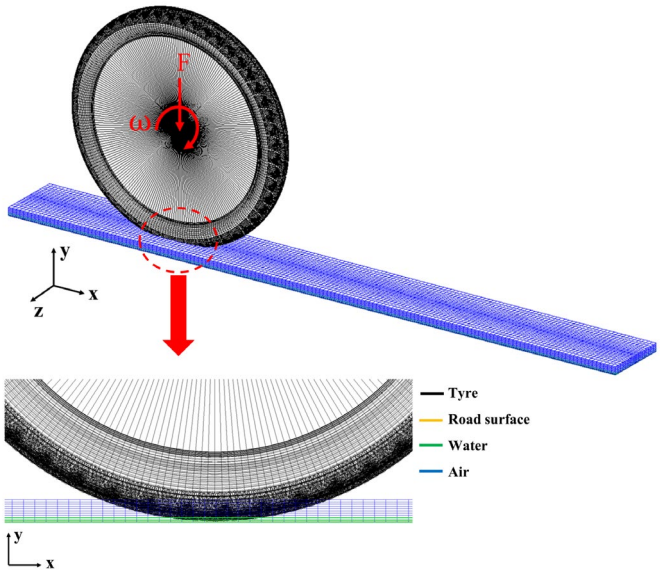

Figure 4. The cell structure of fluid covering the contact surface between tire and road models

EXPERIMENTS

The experiments were performed by two testing types for the motorcycle tire. There were material testing and tire hydroplaning testing. The mechanical properties of the rubber compound for modeling the motorcycle tire model would be obtained by material testing. Meanwhile, tire hydroplaning testing was used to validate the simulation model.

Material Testing

The rubber compound used to manufacture the motorcycle tire is prepared for the C-typed specimens according to ASTM D412, as in Figure 5(a). These specimens performed the tensile test by the universal testing machine according to ASTM D412, shown in Figure 5(b). The testing result obtained from the tensile testing can plot by a graph as shown in Figure 6. Its trend was a logarithm. This trend should fit with the hyperelastic material model. The proper model for the stress-strain behavior of this rubber compound was the penalized first-order Mooney-Rivlin model. It had constants of 0.307 and 1.088 for C_{10} and C_{01}, respectively. The material model fitting was very accurate under the R^2 of 0.95. The belt made of nylon-6 had mechanical properties referred to [19]. It also used the penalized first-order Neo-Hookean model. The constants of the penalized first-order Neo-Hookean model were 90 for C_{10}.

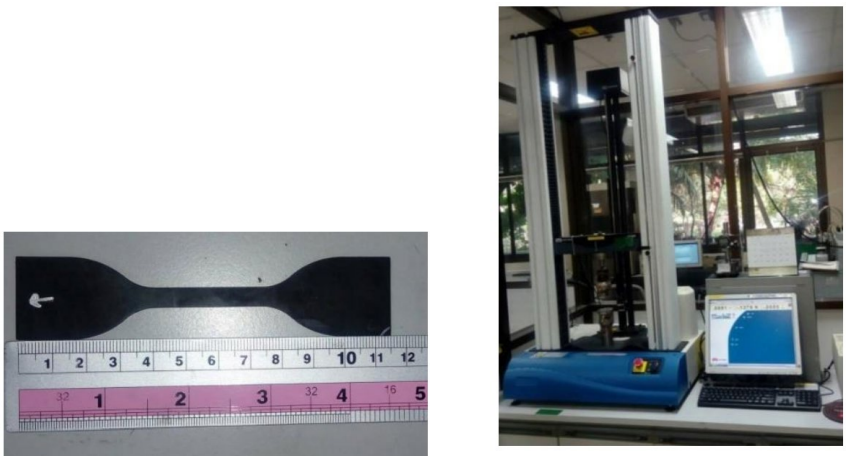

(a) (b)

Figure 5. (a) The C-typed specimen according to the ASTM D412, and (b) the tensile testing of the rubber compound specimen

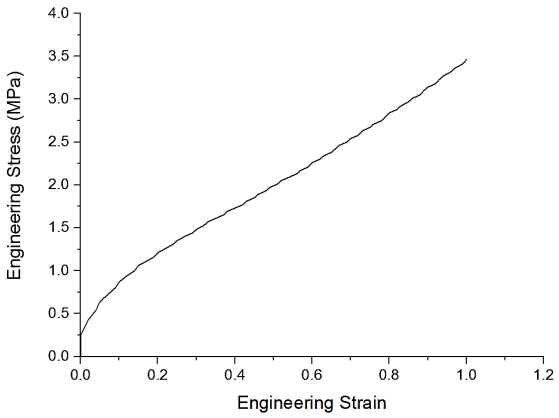

Figure 6. The stress vs. strain graph for the rubber compound of the motorcycle tire

Motorcycle Tire Hydroplaning Testing

Because the hydroplaning force is dangerous to measure by field test; therefore, the invented machine was employed to perform the hydroplaning test in a laboratory instead. The hydroplaning testing on the motorcycle tires had performed by the motorcycle tire hydroplaning testing machine. This machine was fabricated to simulate the motorcycle tire rolling on a dry road and later crushed to the water film on the road. Figure 7 shows the tire hydroplaning testing machine. The runway conveyor was assembled with two drums for the riding road. The motorcycle tire was installed at the arm of the testing machine, which has two axial load cells, as in Figure 8. These were the vertical and horizontal directions of the runway. When the machine arm, which fixed the motorcycle tire, pressed this tire on the conveyor, the motorcycle tire would roll with the desired speed. The ground force was recorded after the tire had the desirable riding velocity and the carrying load. Thenceforth, this machine is controlled to release the water in front of the rolling tire (Figure 9). The water drained on the conveyor was the same as the water film in front of the motorcycle. The rubber ribs had glued at both rims of the conveyor to protect the water leaking from the conveyor. They could help the uniform thickness of water on the conveyor. In addition, the water thickness could calculate from the volume flow rate of water between ribs. The rolling tire would crush and ride on the water film, and the hydroplaning pressure happened under the rolling tire. The load cell, which was installed at the machine arm, measured the ground force. The ground force of the wet conveyor would decrease from the dry conveyor. Therefore, the force, which lifted the rolling tire, was obtained by the different ground force values between dry and wet conveyors. It was the real hydroplaning force, as mentioned above.

Figure 7. The hydroplaning testing machine invented for motorcycle tires

Figure 8. Installation of a motorcycle tire at the machine arm

Figure 9. Water draining on the runway in front of the rolling tire

This study set up the water film at 3.00 mm and the tire speed of 50 km/hr. The weight of a rider riding a motorcycle was the carrying load on the rolling tire. It was 850 N. The inflation pressure of the tire was 250 kPa. Consequently, the ground force graph of a rolling tire on the dry and wet conveyors is continuously plotted and depicted in Figure 10. Repeated testing of tire hydroplaning was performed three times. The carrying load of the rolling tire was reduced distinctly. The decreased value of the carrying load, which was measured by the load cell, was the hydrodynamic force or hydroplaning force. Because the force signals were a sinusoidal curve, the root mean square (RMS) would be used to manipulate these data. Table 1 shows the testing results. It found that the ground force between the tire and runway was different a little from the carrying load. It was caused by the absorption of air inflation pressure. In addition, the translational velocity of the rolling tire would reduce to an average value of 46.32 km/hr. The tire runway friction affected the decrease in translation velocity. Therefore, the average hydroplaning force, which was the different ground force values between dry and wet conveyors, was 64.19 N with a deviation of ±3.50 N.

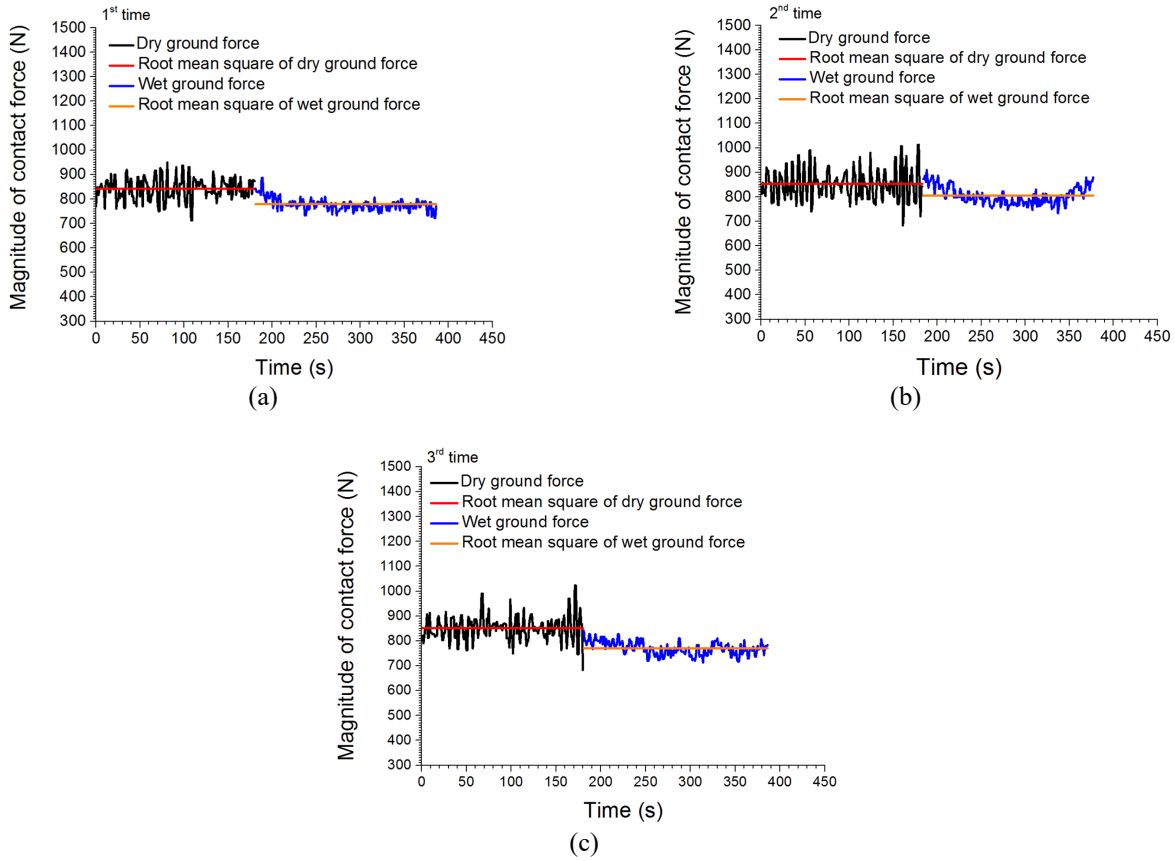

Figure 10. Time history of the contact force of the rolling motorcycle tire on the dry and wet runway at (a) 1st, (b) 2nd, and (c) 3rd testing

Table 1. Experimental results of the motorcycle tire hydroplaning

Testing Time	Velocity (km/hr)	Dry ground force (N)	Wet ground force (N)
1	45.45	842.93	778.79
2	46.77	853.05	806.01
3	46.73	852.25	770.87
Average	46.32	849.41	785.22

RESULTS AND DISCUSSION

Validation

The initial condition of the rolling tire model consisted of the tire speed, inflation pressure, and carrying load. To examine the time response of tire contact force to the road condition and tire model, the tire speed and carrying load were assigned for the same experimental results. The simulation was carried out in the time range of 0.07 seconds. Figure 11 shows the simulation of the rolling tire on a dry road. The stress happening on the rolling tire was represented by the color contour. The highest stress value was red, while the lowest was blue. It was found that the maximum stress occurred on the tire belt. Therefore, it was the nylon-6 which was an important component of a motorcycle tire to support the inflation pressure and the carrying load.

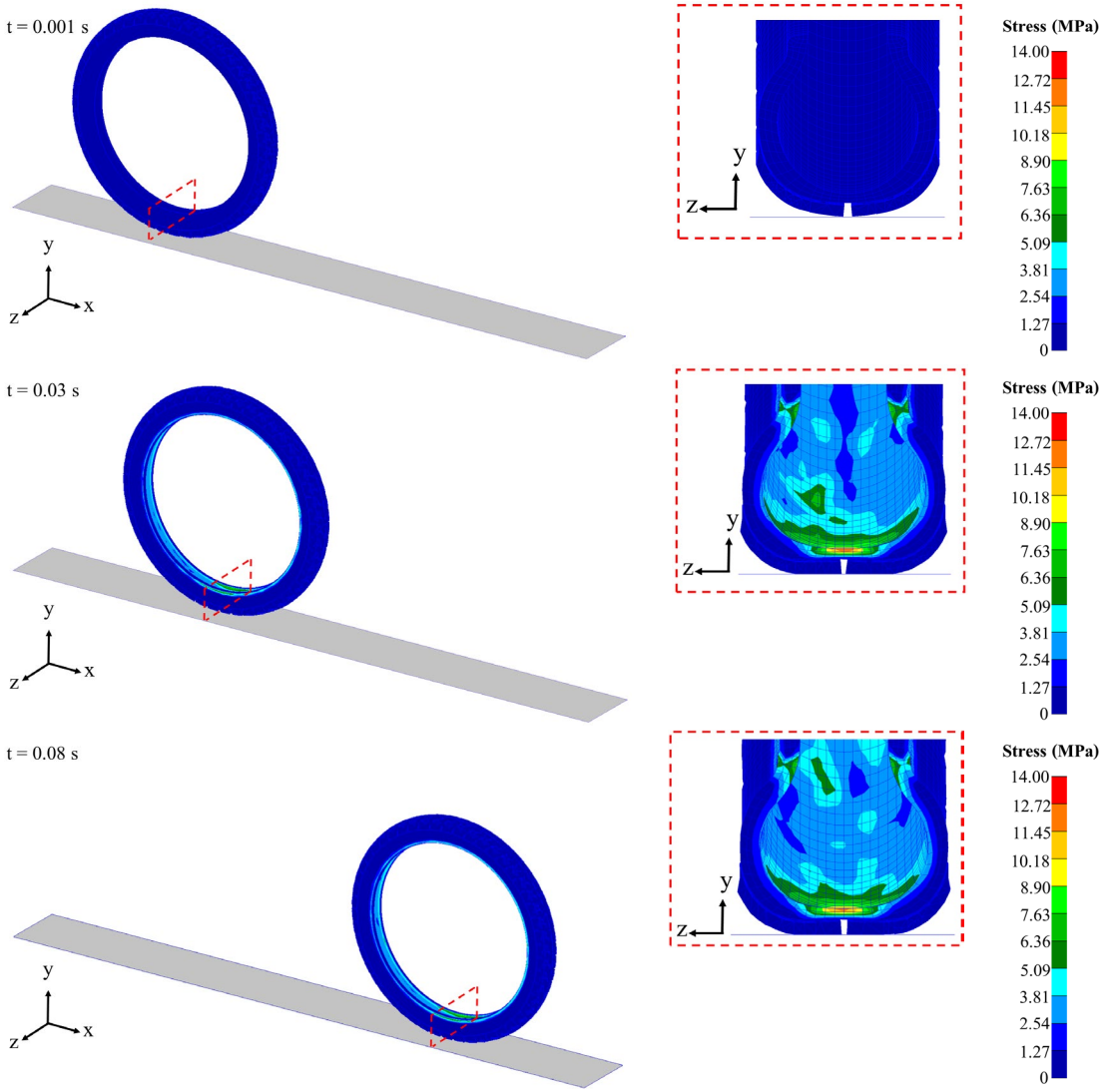

Figure 11. Stress in the section view of the motorcycle tire rolling on a dry road at 0.001, 0.03, and 0.08 seconds

Figure 12 shows the simulation of the rolling tire on the wet road. The stress happening on the rolling tire was also represented by the color contour. The highest stress value was red, while the lowest was blue. It found that the stress values of the rolling tire on the wet road were higher than on the dry road at the same time. However, it was less than the failure stress of the tire belt. The water film on the road was drained off the road by the rolling tire. The general Eulerian-Lagrangian coupling that was the FSI algorithm could calculate the draining water on the wet road by the rolling tire. It is observed clearly by the representation of the water volume fraction, as shown in Figure 13. The water volume fraction

was represented by color contour. Its value was equal to 1.00, which means the finite volume cell was full of water. On the other hand, the cell was full of air when the water fraction value was equal to 0. Some water film was in this rolling tire trace. This tire tread pattern has a good drainage ability of water film on the road.

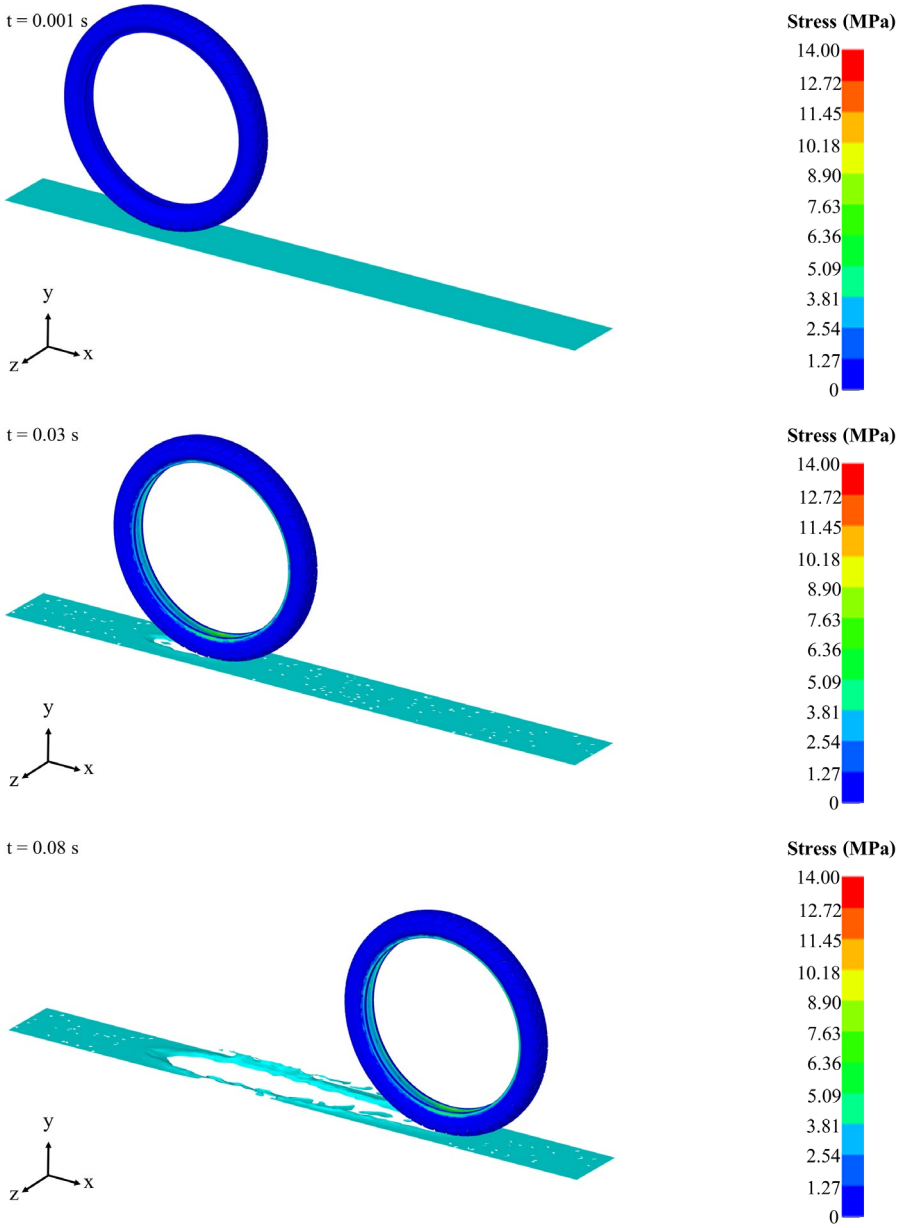

Figure 12. Stress of the motorcycle tire rolling on a wet road at 0.001, 0.03, and 0.08 seconds

Figure 14 shows the vector field of water velocities that drain by the tire tread pattern. It was observed that the water flow was in the lateral direction of the rolling tire at high speed. It came from the circumference groove and to the rib of the tire tread pattern. This pattern could superbly spread water film out of the road surface. In addition, the investigation of water velocities using the FSI algorithm is the advantage method supplementing the design of tire tread patterns to drain the water film on the wet road. This suitable rolling tire model had been used on an Intel CPU Core i7 3.0 GHz with 8 GB of DDR3 RAM. On the wet road, it had been computed in 7 hr. The computational time of the rolling tire on the dry road was less than the rolling tire on the wet road of 3 hr.

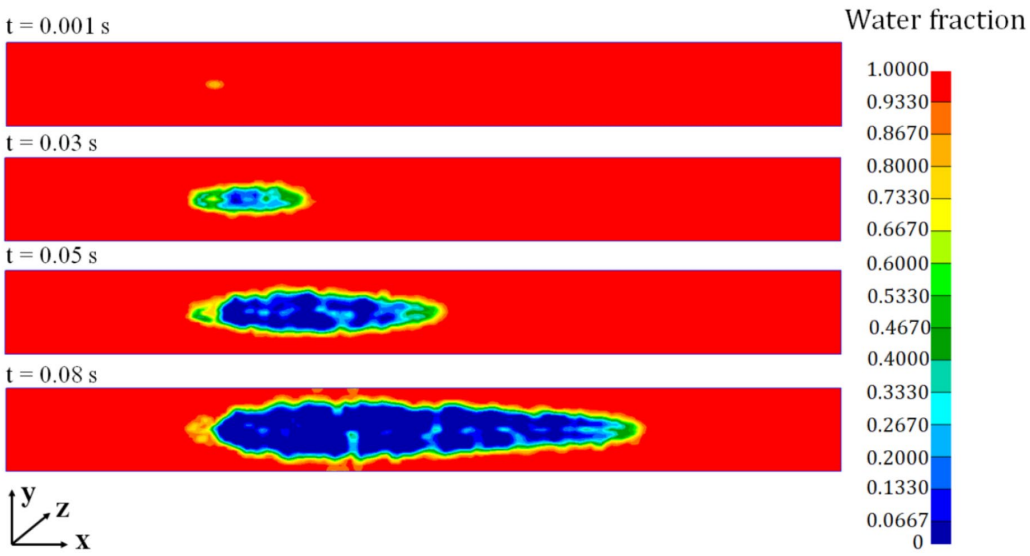

Figure 13. Water volume on the road from the rolling tire at 0.001, 0.03, 0.05, and 0.08 seconds

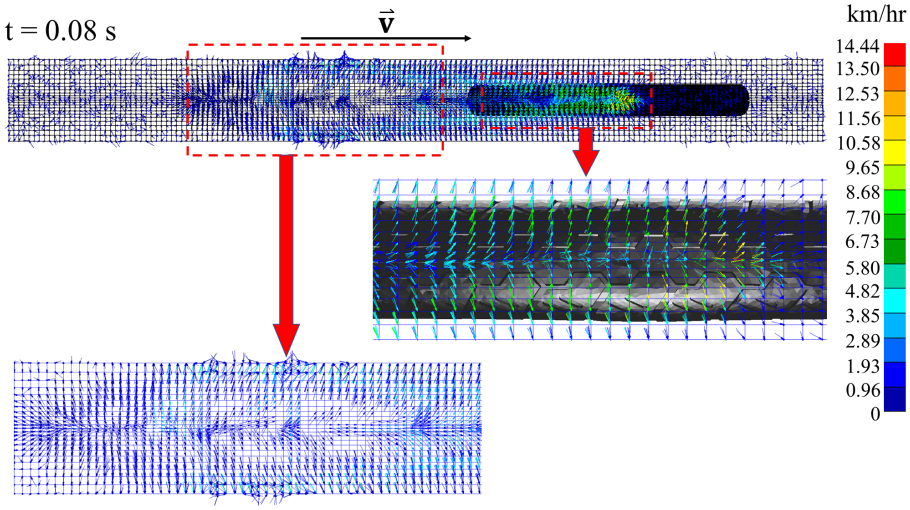

Figure 14. Water film velocity out of the road by the rolling tire at 0.08 seconds

The contact force, which was the interaction force between tire and road, was calculated by the rolling tire on the dry road model. It is initiated by compressing the tire on the dry road at the time of steps 1 to 2 and rolling at the time of step 3, as shown in Figure 15(a). The tire model was placed above the road surface a little. It would impact the road when pressed by the vertical load. Therefore, the contact force shot to 1100 N happened before rolling in step 3 with constant speed. The contact force of the rolling tire on the wet road happens the same as on the dry road at steps 1 to 2, as in Figure 15(b). Its value was reduced by the hydroplaning force observed at the time of step 3. The contact force in this step happened when the tire was rolled. Therefore, its form was in the sinusoidal wave. The time history of contact force between the rolling tire and dry and wet roads in step 3 is compared by the graph to investigate the hydroplaning force (Figure 15(c)). The contact force of the rolling tire on the wet road was decreased distinctly. The hydroplaning pressure happened on the rolling tire, which caused the decrease of ground force or contact force. The RMS was employed to obtain the contact force value of the rolling tire in the time range of step 3. Therefore, the contact forces of dry and wet roads were compared against the carrying load in the experiment. It was in good agreement with the experiment. Table 2 shows the detail of the comparison of contact force between the simulation and experiment. The error in the comparison of contact force between the rolling tire and wet road was more than the dry road. The coupling algorithm between fluid and solid was the main cause of the error. In addition, it was also concerned with the contact algorithm of a rolling tire and a road. However, the accuracy of the hydroplaning rolling tire model was satisfied because the error just was 10.31% for the narrow tire.

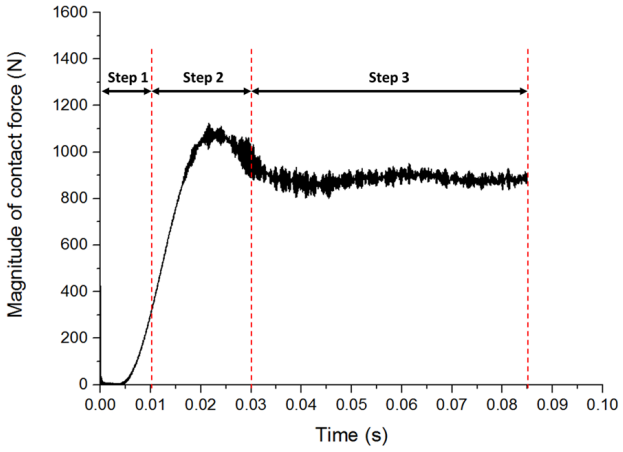

(a)

Figure 15. The contact force between

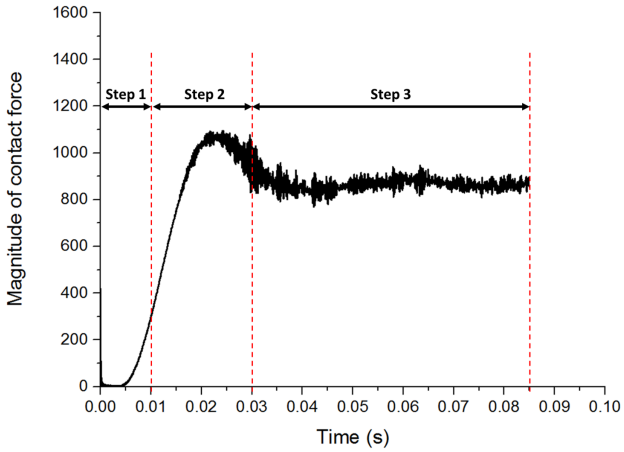

(b)

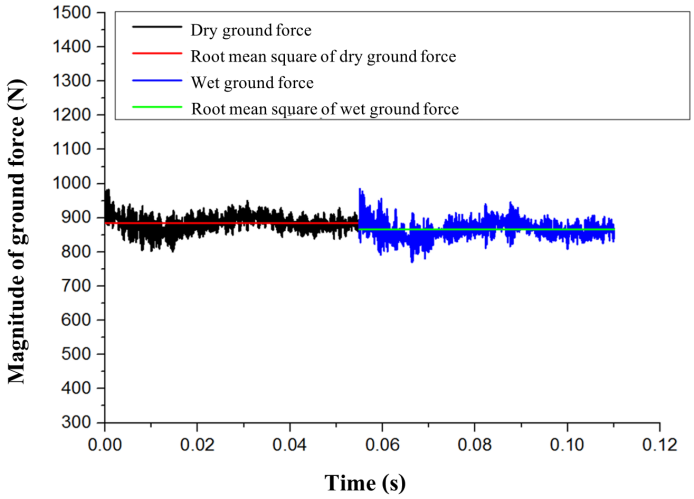

(c)

Figure 15. Contact force between the (a) rolling tire and a dry road, (b) rolling tire and a wet road, and (c) comparison of both contact forces

Table 2. The detail of contact force between the rolling tire and dry and wet roads

Experiment		Simulation		Error (%)	
RMS of contact force between rolling tire and dry road (N)	RMS of contact force between rolling tire and wet road (N)	RMS of contact force between rolling tire and dry road (N)	RMS of contact force between rolling tire and wet road (N)	Dry road	Wet road
849.41	785.22	884.82	866.84	4.17	10.31

Effects of Rolling Tire Speed

The tire speed was increased to study the hydroplaning effect. The setting tire velocities were 40, 50, 60, 70, 80, and 90 km/hr. Meanwhile, the inflation pressure and carrying load were constant at 850 N and 250 kPa, respectively. Figure 16 shows the water drainage of the rolling tire at each speed at a constant time of 0.06 seconds. The water film behind the rolling tire appeared as a trace of the tire. It could not reform the water film because the investigation time was short. However, it could be observed that the water spread to both sides of the rolling tire. The contact force between the rolling tire and both road conditions at each rolling tire speed is plotted by graphs, as shown in Figure 17. The dry road expressed the constant contact force, while the wet road showed a decrease in contact force when the tire speed was increased. The different values of contact forces between the dry and wet roads increased gradually. It means the increase in motorcycle speeds will increase the risk of an accident by hydroplaning. The motorcycle falls when its velocity induces the contact force close to zero.

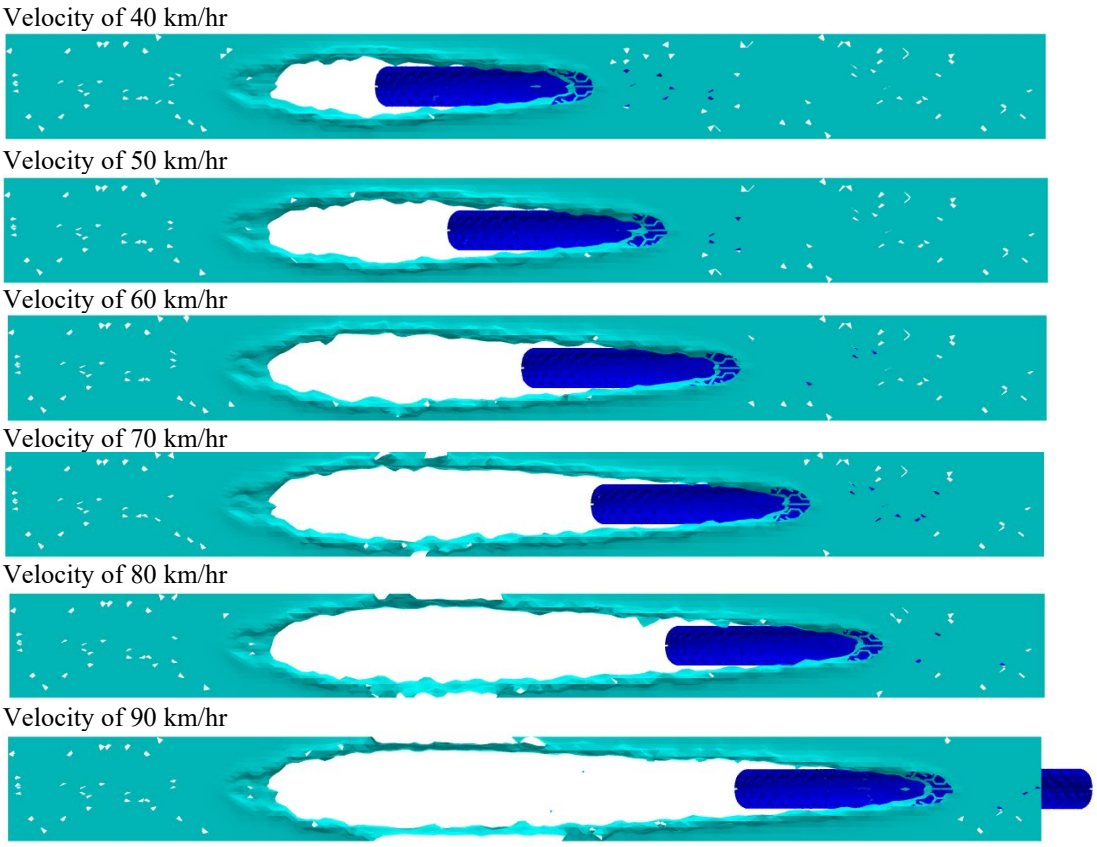

Figure 16. Water film on the road surface spreads at the rolling tire speed from 40 to 90 km/hr with an interval of 10 km/hr

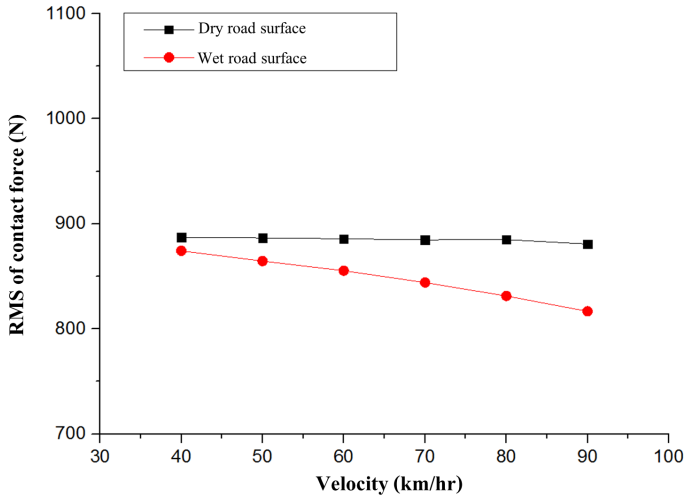

Figure 17. Root mean square of contact force vs velocity of the rolling tire on the dry and wet roads

Effects of Carrying Load

The effects of carrying load on the contact force between the rolling tire and both roads were investigated. The carrying load consisted of 860, 910, 960, 1010, 1160, 1110, 1160, 1210, and 1260 N, while the rolling tire velocity and inflation pressure were at 90 km/hr and 250 kPa, respectively. The range of carrying loads was using the motorcycle tire with a rider and passenger. This tire weight was 10 N. The water film is drained off the road surface by the rolling tire with different carrying loads in Figure 18. The drained water was shown distinctly by the water's surface. It was found that the water flow was a little different shape on the road surface. The contact force on the dry and wet roads with different carrying loads is plotted in Figure 19. The increase in contact force followed the increase in carried load. The different contact force values on both roads were increased a little in the carrying load range of the investigation.

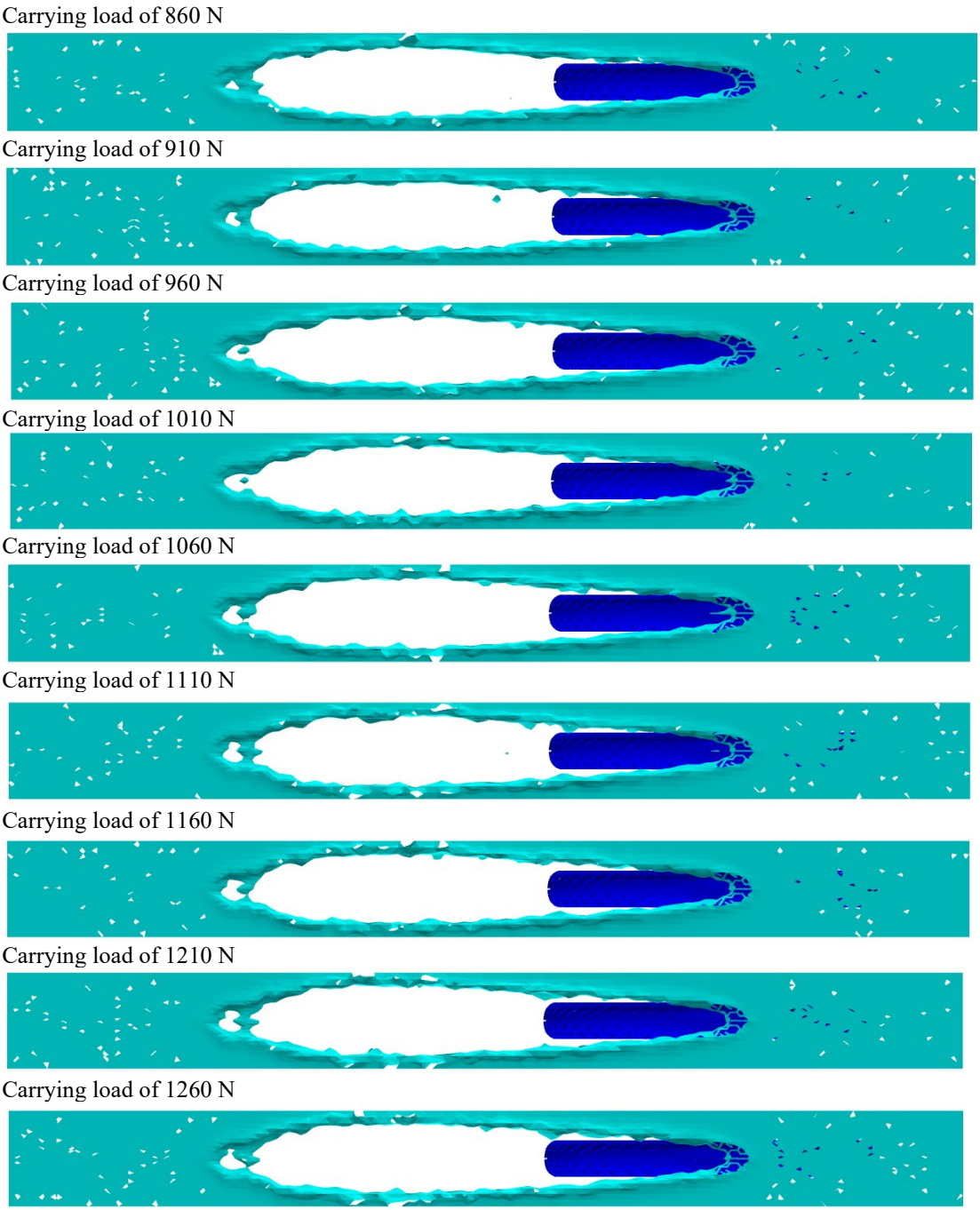

Figure 18. Water film on the road surface spreads by rolling tires with different carrying loads at a velocity of 90 km/hr

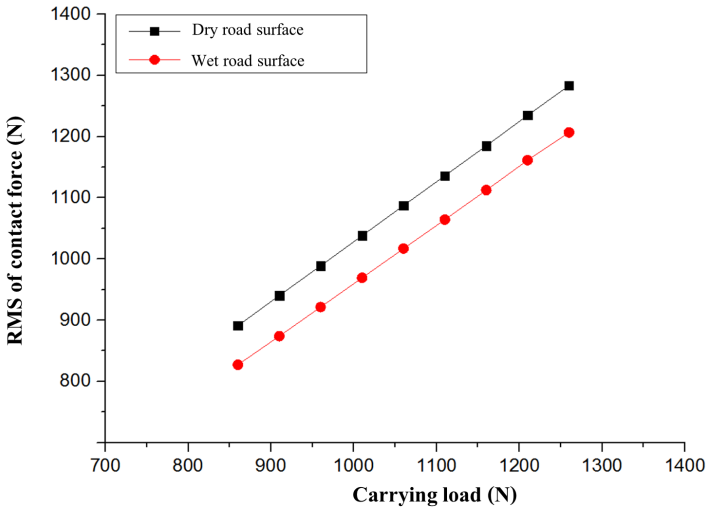

Figure 19. Root mean square of contact force vs carrying load of the rolling tire on the dry and wet roads

Effects of Air Inflation Pressure

To investigate the inflation pressure effect on the contact force, the rolling tire velocity and the carrying load were constant at 90 km/hr and 860 N, respectively. The inflation pressure of the rolling tire varied from 170 to 250 kPa with an interval of 20 kPa. These investigating pressure values were in the usage range of the motorcycle tire. Figure 20 shows the water film spreads by the rolling tire with different inflation pressures with slightly different shapes at the same time. The contact force on both road conditions with the different values of inflation pressure of the rolling tire is plotted by graphs, as shown in Figure 21. It was observed that the inflation pressure unaffected the contact force between the tire and the road. The contact force was constant when the inflation pressure was increased. The sidewall deformation of the motorcycle tire occurred instead of the tire tread deformation when the inflation pressure was varied. These caused the contact patch of the rolling tire to be unchangeable. Figure 22 shows the tire deformation at various inflation pressures while the carrying load is maximum and the rolling tire is initial. The color contour of displacement for each inflation pressure was close. The simulation result could examine this significant phenomenon of rolling motorcycle tires.

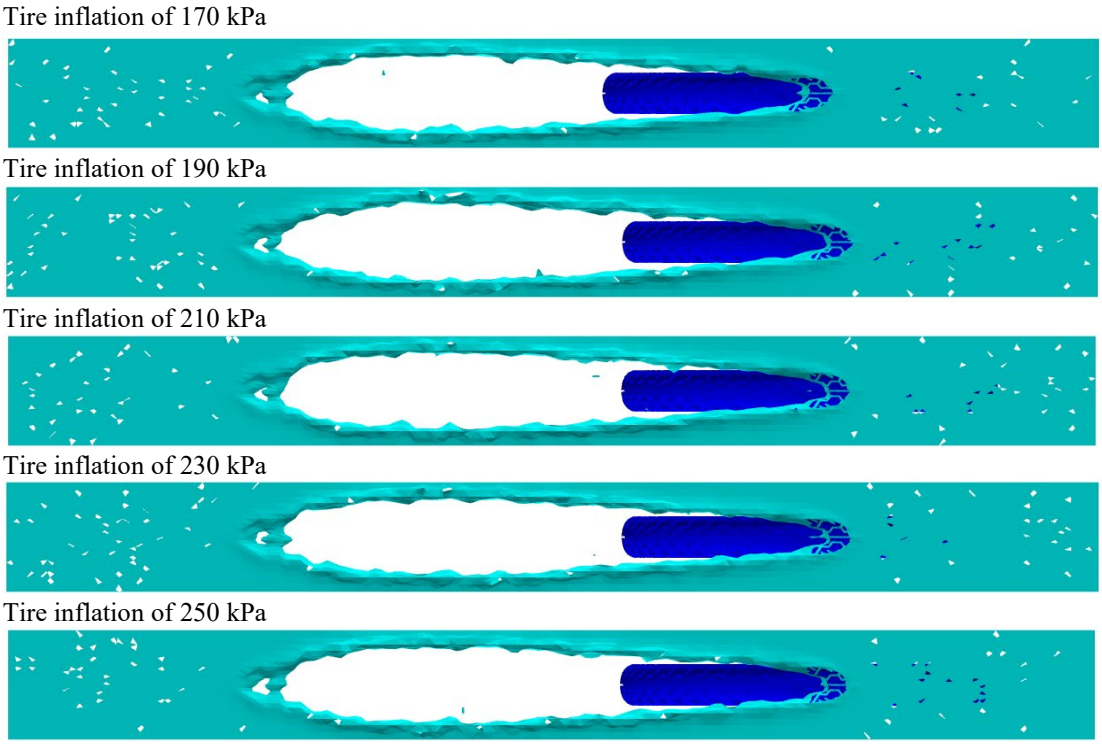

Figure 20. Water film on the road surface spreads by rolling tires with different inflation pressures at a velocity of 90 km/hr

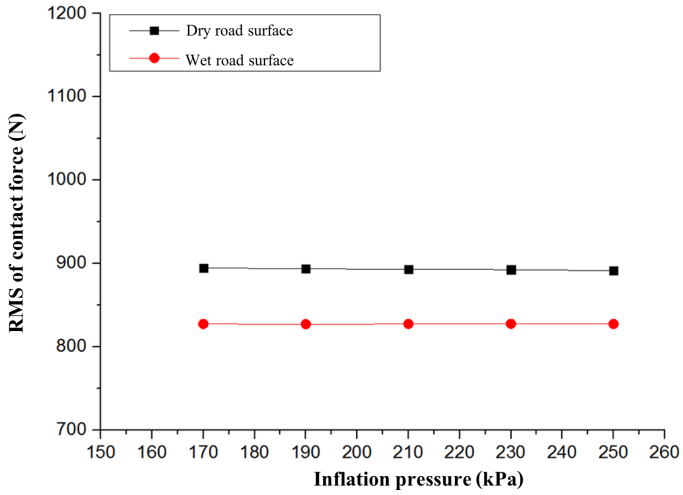

Figure 21. Root mean square of contact force vs inflation pressure of the rolling tires on the dry and wet roads

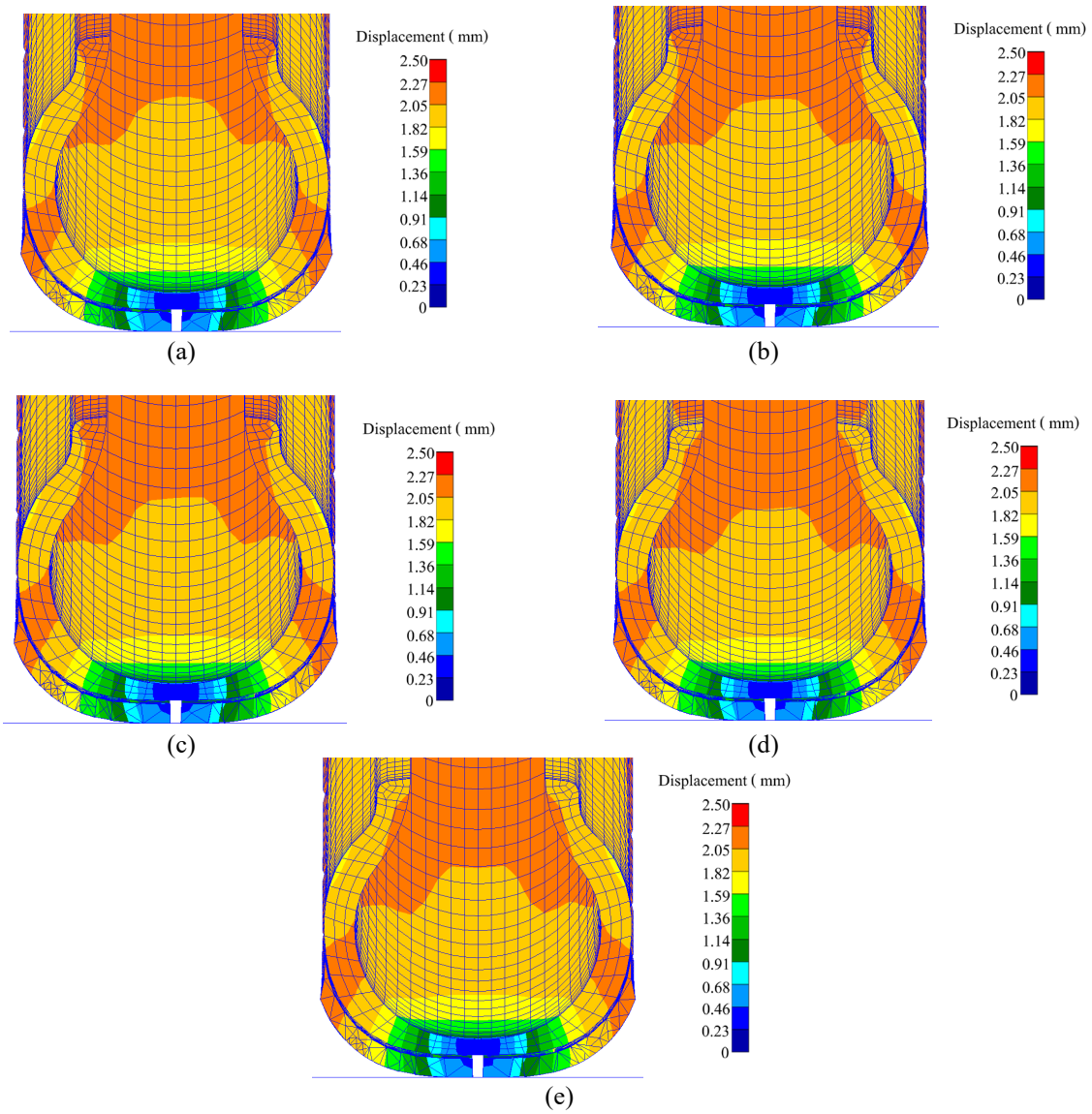

Figure 22. Tire deformation at the initial time of rolling at a velocity of 90 km/hr (0.01 seconds), a maximum carrying load of 860 N, and varying inflation pressures of (a) 170 N, (b) 190 N, (c) 210 N, (d) 230 N, and (e) 250 N

Hydroplaning Speed Equations of Motorcycle Tire

The hydrodynamic force or hydroplaning force can be obtained from the different contact forces between the rolling tire on dry and wet roads. It is increased gradually by the increase of tire velocity. Figure 23 shows the effect of tire velocity on the hydroplaning force. The relation between the hydroplaning forces and rolling tire velocities was linear and can be written by Eq. (22).

$$F_h = aV_h + b \tag{22}$$

where F_h is the hydroplaning force, V_h is the hydroplaning tire speed, and a and b are constant values. When the constant value of a and b was 1.033 and -29.89, respectively, the hydroplaning function had an R^2 of 0.99. The linear relation between hydroplaning force and velocity differs from the hydroplaning force in literature [20].

The hydroplaning force was affected by the increase in carrying loads. The relationship between the hydroplaning force and the carrying load is linear (as in Figure 24). The linear function, which governs the effect of increasing the carrying load on the hydroplaning force, is written in Eq. (23).

$$F_h = cL_c + d \tag{23}$$

where F_h is the hydroplaning force, L_c is the carrying load, and c and d are constant values. The constant value of c and d was 0.027 and 41.16, respectively. Therefore, the hydroplaning function, which depended on the carrying load, had an R^2 of 0.98. The simulation results amazed the inflation pressure effect on the hydroplaning force. The hydroplaning force was unaffected by the increase in inflation pressure. Therefore, it was inconsiderable to establish the hydroplaning speed equation. Equation (22) is equal to Eq. (23). The hydroplaning speed equation is written as follows:

$$V_h = DL_c + P \tag{24}$$

where F_h is the hydroplaning force, L_c is the carrying load, and D and P are constant values.

This function was proposed instead of the previous hydroplaning speed equation of literature. It was different because it depended just on the carrying load. In addition, it is easy to implement. The tire performance for the hydroplaning speed can determine when the riders predict the carrying load. Therefore, they should be aware of the critical speed while riding a motorcycle on a wet road. Although a more carrying load causes a high hydroplaning speed, the limitation of the carrying load for this tire should concern for riding. The constants D and P are 0.028 and 69.88 for the 2.25-17 motorcycle tire, respectively.

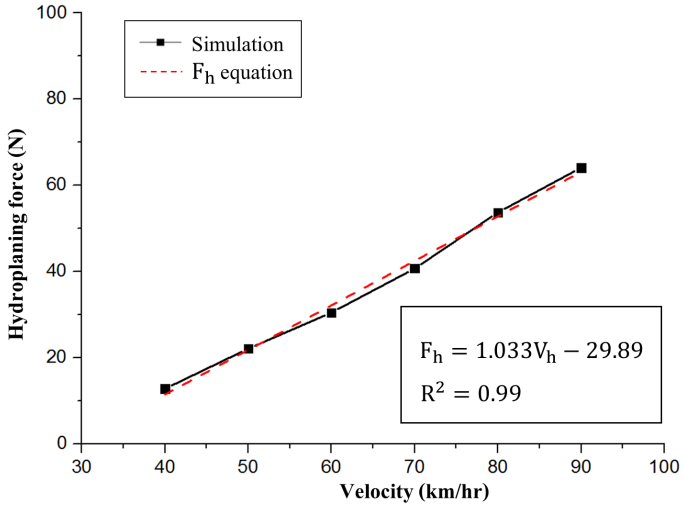

Figure 23. Hydroplaning force vs velocity of the rolling tire on a wet road

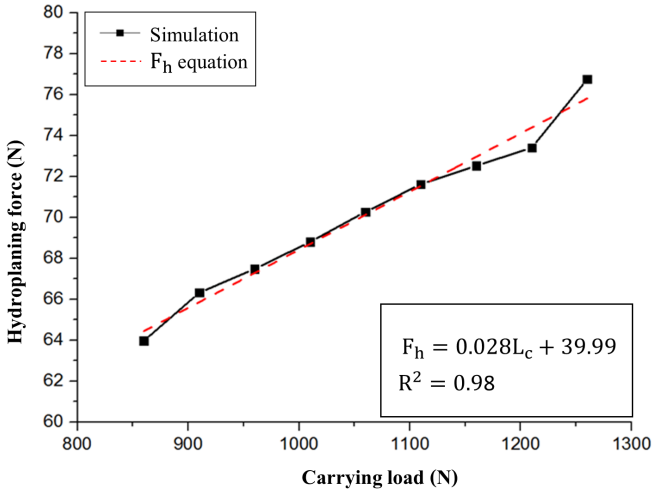

Figure 24. Hydroplaning force vs inflation pressure of the rolling tire on dry and wet roads

CONCLUSIONS

The rolling tire hydroplaning of motorcycles was investigated because they are easy to have an accident, and severe accidents often happen to motorcycle riders. The study of hydroplaning was carried out by both experiment and simulation. This study has never been performed even though it is useful and safe for commuters. The studied results are concluded as follows:

i. The motorcycle tire was performed dynamic testing by rolling on dry and wet roads. The experiment showed that the water film on the wet road generated hydroplaning pressure between the rolling tire tread and the road. The hydroplaning force was measured by the tire hydroplaning testing machine, where the difference in carrying load between the rolling tire on dry and wet roads is the hydroplaning force.

ii. The simulation used finite element and finite volume methods to model the rolling tire and fluid. The interaction of the tire and both fluids was used in the general Eulerian-Lagrangian coupling algorithm. It could calculate contact force while the water surface varied all time caused by the rolling tire tread. The simulation model was satisfied by the experiment. It was found that the rolling tire model on dry and wet roads had an average error of 4.17% and 10.31%, respectively. The complexity and the thin water film of the rolling tires on the wet road increased the simulational error.

iii. The simulation results showed that the hydroplaning force increased gradually to the tire velocity and the carrying load. Meanwhile, the inflation pressure unaffected the hydroplaning force. It just forced the deformation of the tire sidewall so that the contact patch was not variable.

iv. The novel equation of hydroplaning velocity of motorcycle tires was proposed in the carrying load variable form. It can easily be done by substituting rider and motorcycle weight to know the limitation of hydroplaning velocity. The tire tread patterns, which affect the velocity hydroplaning, are outside the scope of this study. However, it will be studied for the development of hydroplaning velocity equations of various motorcycle tire tread patterns in further works.

ACKNOWLEDGEMENT

This research was funded by The Thailand Research Fund (TRF) and N.D. Rubber Public Co., Ltd. under Research and Researchers for Industry Program, Grant No. PHD59I0090.

REFERENCES

[1] W. B. Horne, U. Joyner and T. J. Leland,"Study of the retardation force developed on an aircraft tire rolling in rush or water," 1960. [Online]. Available: https://ntrs.nasa.gov/api/citations/20010057773/downloads/20010057773.pdf. [Accessed: Jan. 11, 2023].

[2] W. C. Horne and T. J. W. Leland,"Influence of tire tread pattern and runway surface condition on breaking friction and rolling resistance of a modern aircraft tire," 1962. [Online]. Available: https://ntrs.nasa.gov/api/citations/19620005764/downloads/19620005764.pdf. [Accessed: Jan. 11, 2023].

[3] W. C. Horne and R. C. Dreher,"Phenomena of pneumatic tire hydroplaning," 1963. [Online]. Available: https://ntrs.nasa.gov/api/citations/19640000612/downloads/19640000612.pdf. [Accessed: Jan. 11, 2023].

[4] M. Zmindak and I. Grajciar, "Simulation of the aquaplane problem," *Computers & Structures*, vol. 64, no. 5/6, pp. 1155–1164, 1997.

[5] Y. Nakajima, E. Seta, T. Kamegawa, and H. Ogawa, "Hydroplaning analysis by FEM and FVM – effect of tire rolling and tire pattern on hydroplaning," *International Journal of Automotive Technology*, vol. 1, no. 1, pp. 26–34, 2000.

[6] Y. Nakajima, *Advanced Tire Mechanics: volume 2*, Singapore: Springer, 2019.

[7] J. R. Cho, H. W. Lee, J. S. Sohn, G. J. Kim, and J. S. Woo, "Numerical investigation of hydroplaning characteristics of three-dimensional patterned tire," *European Journal of Mechanics - A/Solids*, vol. 25, no. 6, pp. 914–926, 2006.

[8] J. Sapragonas, A. Kersys, and R. Makaras, V. Lukosevicius, and D. Juodvalkis, "Research of the influence of tire hydroplaning on directional stability of vehicle," *Transport*, vol. 28, no. 4, pp. 374–380, 2013.

[9] J. Y. Jeong and H. Y. Jeong, "Hydroplaning simulation of a tire in thin water using FEM and an estimation method and its application to skid number estimation," *International Journal of Automotive Technology*, vol. 14, no. 2, pp. 325–331, 2013.

[10] X. Zhu, Y. Pang, J. Yang, and H. Zhao, "Numerical analysis of hydroplaning behaviour by using a tire-water-film-runway model," *International Journal of Pavement Engineering*, vol. 23, no. 3, pp. 784-800, 2022.

[11] X. Zhang, F. Xu, X. Ren, X. Gao, and R, Cao, "Consideration on aircraft tire spray when running on wet runways," *Chinese Journal of Aeronautics*, vol. 33, no. 2, pp. 520–528, 2020.

[12] C. Liang, L. Ji, H. Mousavi, and C. Sandu, "Evaluation of tire traction performance on dry surface based on tire-road contact stress," in *The 30th SIAR International Congress of Automotive and Transport Engineering, SMAT 2019*, I. Dumitru, D. Covaciu, L. Racila, A. Rosca, Eds. Switzerland, Springer, 2020, pp. 138–152.

[13] J. Phromjan and C. Suvanjumrat, "Development of solid tire model for finite element analysis of compressive loading," *Songklanakarin Journal of Science and Technology*, vol. 43, no. 1, pp. 229–236, 2021.

[14] C. Liu, G. Wang, H. Zhou, Y. Mei, Y. Li, and L. Zhang, "Design of two-wheeled motorcycle tire crown contour bioinspired by cat paw pads," *Applied Bionics and Biomechanics*, vol. 2020, pp.1-10, 2020.

[15] C. Suvanjumrat, "Comparison of turbulence models for flow past NACA0015 airfoil using OpenFOAM," *Engineering Journal*, vol. 21, no. 3, pp. 207–221, 2017.

[16] K. Loksupapaiboon and C. Suvanjumrat, "Effects of flow and heat transfer around a hand-shaped former," *Engineering Applications of Computational Fluid Mechanics*, vol. 16, no. 1, pp. 1619–1640, 2022.

[17] E. Chaichanasiri and C. Suvanjumrat,"Simulation of three dimension liquid-sloshing models using C++ open source code CFD software," *Kasetsart Journal - Natural Science*, vol. 46, no. 2, pp. 978–995, 2012.
[18] S. B. Rayhan, X. Pu, and X. Huilong," Modeling of fuel in crashworthiness study of aircraft with auxiliary fuel tank," *International Journal of Impact Engineering*, vol. 161, 2022.
[19] T. Varaporn and S. Nutthorn,"Rubber toughening of nylon 6 with epoxidized natural rubber," *Polymer Testing*, vol. 27, pp. 794-800, 2008.
[20] F. Spitzhüttl, F. Goizet, T. Unger, and F. Biesse," The real impact of full hydroplaning on driving safety," *Accident Analysis & Prevention*, vol. 138, p.105458, 2020.